Calcium Dynamics Associated with a Single Action Potential in a CNS Presynaptic Terminal

Fritjof Helmchen, J. Gerard G. Borst, and Bert Sakmann
Abteilung Zellphysiologie, Max-Planck-Institut für medizinische Forschung, 69120 Heidelberg, Germany

ABSTRACT Calcium dynamics associated with a single action potential were studied quantitatively in the calyx of Held, a large presynaptic terminal in the rat brainstem. Terminals were loaded with different concentrations of high- or low-affinity Ca^{2+} indicators via patch pipettes. Spatially averaged Ca^{2+} signals were measured fluorometrically and analyzed on the basis of a single compartment model. A single action potential led to a total Ca^{2+} influx of 0.8–1 pC. The accessible volume of the terminal was about 0.4 pl; thus the total calcium concentration increased by 10–13 μM. The Ca^{2+}-binding ratio of the endogenous buffer was about 40, as estimated from the competition with Fura-2, indicating that 2.5% of the total calcium remained free. This is consistent with the peak increase in free calcium concentration of about 400 nM, which was measured directly with MagFura-2. The decay of the $[Ca^{2+}]_i$ transients was fast, with time constants of 100 ms at 23°C and 45 ms at 35°C, indicating Ca^{2+} extrusion rates of 400 and 900 s^{-1}, respectively. The combination of the relatively low endogenous Ca^{2+}-binding ratio and the high rate of Ca^{2+} extrusion provides an efficient mechanism for rapidly removing the large Ca^{2+} load of the terminal evoked by an action potential.

INTRODUCTION

Calcium ions in presynaptic nerve terminals control transmitter release, as well as several types of short-term synaptic plasticity (Smith and Augustine, 1988; Zucker, 1994). During a presynaptic action potential Ca^{2+} channels open for less than a millisecond (Llinás et al., 1982; Borst and Sakmann, 1996). This causes brief, localized domains of high concentrations of intracellular free calcium ($[Ca^{2+}]_i$), which trigger exocytosis of neurotransmitter-containing vesicles, presumably through binding of calcium to a low-affinity receptor (Augustine and Neher, 1992; Schweizer et al., 1995). After the closure of the Ca^{2+} channels, the domains of high $[Ca^{2+}]_i$ rapidly collapse and the calcium ions redistribute within the terminal by diffusion and binding to calcium buffers (Simon and Llinás, 1985; Fogelson and Zucker, 1985; Roberts, 1994). Finally, calcium is removed from the terminal cytoplasm via Ca^{2+} transporters (Blaustein, 1988).

Most of the studies on presynaptic calcium dynamics that used optical detection methods focused on the dynamics of the volume-averaged residual free calcium, because more localized and rapid calcium signals at present are difficult to measure (but see Llinás et al., 1992). The dynamics of the residual free calcium can be described by a single compartment model in which spatial inhomogeneities are neglected (Neher and Augustine, 1992; Tank et al., 1995; Helmchen et al., 1996). In this model Ca^{2+} is captured by a fast endogenous buffer and extruded via a nonsaturable pump. The Ca^{2+} indicator itself is taken into account as a second, exogenous buffer. Varying the amount of the indicator is a method of elucidating the endogenous buffering and extrusion mechanisms (Neher, 1995). In addition, indicator dye overload of a cellular compartment can be used to measure Ca^{2+} fluxes (Schneggenburger et al., 1993; Neher, 1995).

There are few reports of Ca^{2+} signals measured in individual central nervous system (CNS) presynaptic terminals in brain slices (Jackson et al., 1991; Regehr and Tank, 1991; Regehr et al., 1994; Borst et al., 1995). Alternatively, fluorescence signals from pools of labeled terminals were used to characterize presynaptic calcium dynamics at central synapses (Regehr et al., 1994; Wu and Saggau, 1994; Regehr and Atluri, 1995). However, in this type of experiment the concentration of the indicator dye cannot be controlled well and quantitative measurements of $[Ca^{2+}]_i$ are difficult because of the contribution of axons and unstimulated terminals to the fluorescence signal. Recently whole-cell recordings were made from large individual nerve terminals in the medial nucleus of the trapezoid body (MNTB) in slices of rat brainstem (Forsythe, 1994; Borst et al., 1995). In Borst et al. (1995) we reported that single action potentials evoked presynaptic $[Ca^{2+}]_i$ transients, the size and duration of which depended on the concentration of the indicator dye calcium green-5N. Here we extend this study by measuring presynaptic $[Ca^{2+}]_i$ transients using Fura-2, MagFura-2, and calcium orange-5N, and we describe the dynamics of residual free calcium quantitatively according to a single-compartment model. We were particularly interested in determining the ratio of bound Ca^{2+} versus free Ca^{2+} (the endogenous Ca^{2+}-binding ratio) and the rate of Ca^{2+} extrusion, to find out how a presynaptic terminal copes with the Ca^{2+} load evoked by an action potential.

Received for publication 7 October 1996 and in final form 12 December 1996.

Address reprint requests to Dr. Bert Sakmann, Abteilung Zellphysiologie, Max-Planck-Institut für medizinische Forschung, Jahnstr. 29, D-69120, Heidelberg, Germany. Tel.: 49-6221-486-460; Fax: 49-6221-486-459.

0006-3495/97/03/1458/14 $2.00

MATERIALS AND METHODS

Brain slice preparation and electrophysiology

Slices from the brainstem of 8- to 10-day-old Wistar rats were prepared as described previously (Borst et al., 1995). Briefly, rats were decapitated, and 200-μm-thick transverse slices containing the MNTB were cut in ice-cold solution with a vibratome (Campden Instruments, Loughborough, England). The solution for slicing contained (in mM): 125 NaCl, 2.5 KCl, 3 $MgCl_2$, 0.1 $CaCl_2$, 25 dextrose, 1.25 NaH_2PO_4, 0.4 ascorbic acid, 3 *myo*-inositol, 2 sodium pyruvate, and 25 $NaHCO_3$, pH 7.4, when bubbled with carbogen (95% O_2, 5% CO_2). Slices were incubated for 30 min at 37°C in a solution similar to that used for slicing, but containing 2 mM $CaCl_2$ and 1 mM $MgCl_2$, and they were stored at room temperature (22–24°C) thereafter. The same solution (either at room temperature or prewarmed to 35°C) was used to continuously superfuse slices in the recording chamber at 1–3 ml min^{-1}.

Slices were mounted on an upright epifluorescence microscope (Axioskop FS; Zeiss, Oberkochen, Germany) equipped with a 60× water-immersion objective (NA 0.9; Olympus, Tokyo, Japan). Terminals were visualized with an additional twofold magnification (Optovar; Zeiss) using infrared differential interference contrast (IR-DIC) video microscopy (Fig. 1 *A*; Stuart et al., 1993). Tight-seal whole-cell recordings from terminals were made with thick-walled borosilicate glass pipettes (6–11 MΩ resistance) containing (in mM): 115 potassium gluconate, 20 KCl, 4 MgATP, 10 disodium phosphocreatine, 0.3 GTP, 10 HEPES, pH 7.2, adjusted with KOH. The Ca^{2+} indicator dyes Fura-2, MagFura-2 or calcium orange-5N (Molecular Probes, Portland, OR) were added to the pipette solution at different concentrations as noted. Presynaptic recordings were made with one pipette, except in voltage-clamp experiments, in which two pipettes were used.

Voltage recordings were made with an Axoclamp-2B amplifier (Axon Instruments, Foster City, CA), filtered at 5 kHz, and digitized at 10–20 kHz. Ca^{2+} current recordings from calyces were made with an Axopatch-200A amplifier (Axon Instruments). Ca^{2+} currents were isolated pharmacologically. K^+ currents were blocked by replacement of K^+ with Cs^+ in the intracellular solution and replacement of 20 mM NaCl with 20 mM tetraethylammonium chloride (Sigma, St. Louis, MO) plus 0.1 mM 3,4-diaminopyridine (Sigma) in the extracellular solution. Na^+ currents were blocked with 1 μM tetrodotoxin. Series resistance (<26 MΩ) compensation was set at 95% with a lag of 10 μs. Currents were filtered at 3 kHz and sampled at 20 kHz. To check the accuracy of the voltage clamp the membrane potential was monitored with a second pipette in current-clamp mode (Fig. 1, *A* and *B*; Borst et al., 1995). Voltages and currents were digitized on a VMEbus computer system (Delta series 1147; Motorola, Tampa, FL) or with Pulse Control version 4.6 (Herrington and Bookman, 1994) and a 16-bit A/D converter (ITC-16; Instrutech, Great Neck, NY).

Terminals typically had resting membrane potentials between −75 and −80 mV and input resistances higher than 300 MΩ. Potentials were corrected for a junction potential of −11 mV between the extracellular and the pipette solution. A bipolar electrode placed in the trapezoid body at the midline was used for orthodromic stimulation (6–25 V, 50 μs). A patch pipette that recorded extracellular currents close to MNTB synapses was used to find presynaptic terminals that responded to orthodromic stimulation (Borst et al., 1995). No preselection was made in experiments in which the calibration constants R_{min}, K_{eff}, or f_{max} were determined. Orthodromically evoked presynaptic action potentials (Fig. 1 *C*) had amplitudes around 100 mV, and half-widths of 0.58 ms and 0.26 ms at room temperature and 35°C, respectively, and were followed by a depolarizing afterpotential, as previously described (Borst et al., 1995).

Single compartment model of the terminal

Fluorescence signals of the Ca^{2+} indicators were collected from the whole terminal; therefore they represent spatially averaged cytosolic Ca^{2+} signals (Fig. 1 *B*). They were analyzed according to a single compartment model (Neher and Augustine, 1992; Tank et al., 1995; Helmchen et al., 1996). This model assumes instantaneous Ca^{2+} influx and neglects spatial inhomogeneities. For a discussion of the validity of the assumptions see the Appendix. During a presynaptic action potential a Ca^{2+} current I_{Ca} with a total charge of $Q_{Ca} = -\int I_{Ca}\,dt$ flows into the terminal. The initial increase of the average total Ca^{2+} concentration ($\Delta[Ca]_T$) is given by $Q_{Ca}/(2\,FV)$, where F is the Faraday constant and V is the volume accessible to Ca^{2+}. Calcium is assumed to bind to a fast, endogenous buffer (S). The Ca^{2+}-binding capacity of this buffer is given as the Ca^{2+}-binding ratio $\kappa_S = \partial[CaS]/\partial[Ca^{2+}]_i$. The exogenously added Ca^{2+} indicator (B) competes with the endogenous buffer (S) and as a result affects size and duration of the $[Ca^{2+}]_i$ transients. For data analysis the incremental binding ratio κ'_B is used (Neher and Augustine, 1992):

$$\kappa'_B = \frac{\Delta[CaB]}{\Delta[Ca^{2+}]_i} = \frac{[B]_T K_d}{([Ca^{2+}]_{rest} + K_d)([Ca^{2+}]_{peak} + K_d)}. \quad (1)$$

$[Ca^{2+}]_{rest}$ is the free Ca^{2+} concentration at rest, and $[Ca^{2+}]_{peak} = [Ca^{2+}]_{rest} + \Delta[Ca^{2+}]_i$. $[B]_T$ is the concentration and K_d the dissociation constant of the indicator. For low-affinity indicators and small changes in $[Ca^{2+}]_i$, Eq. 1 simplifies to $\kappa'_B = [B]_T/K_d$. Ca^{2+} removal is modeled as a linear extrusion mechanism with a rate constant γ:

$$\left(\frac{d[Ca]_T}{dt}\right)_{out} = -\gamma([Ca^{2+}]_i - [Ca^{2+}]_{rest}) = -\gamma\Delta[Ca^{2+}]_i. \quad (2)$$

The removal system may include extrusion via the plasma membrane, uptake into intracellular organelles, or slow binding to cytoplasmic buffers (Sala and Hernández-Cruz, 1990; Neher and Augustine, 1992). Exchange of free and bound Ca^{2+} with the pipette solution is neglected, because this occurs on a time scale of minutes (Fig. 2 *A*; Borst et al., 1995). The $[Ca^{2+}]_i$ transient evoked by a single action potential is described by an exponential curve with amplitude A and decay time constant τ (Helmchen et al., 1996):

$$A = \frac{Q_{Ca}/(2FV)}{(1 + \kappa'_B + \kappa_S)}, \quad \tau = \frac{1 + \kappa'_B + \kappa_S}{\gamma}. \quad (3)$$

The time constant and the inverse of the amplitude depend linearly on the exogenously added Ca^{2+}-binding ratio κ'_B. Measuring these relationships makes it possible to estimate A and τ in the absence of exogenous buffers by extrapolation to $\kappa'_B = 0$. Estimates of the endogenous Ca^{2+}-binding ratio κ_S can be obtained from the negative x axis intercepts of the plots of A^{-1} and τ versus κ'_B, which are equal to $1 + \kappa_S$ (Neher and Augustine, 1992).

Fluorescence measurements

A polychromatic illumination system was used for excitation (T.I.L.L. Photonics, Munich, Germany). Fura-2 was excited at 357 nm (isosbestic) and 385 nm for ratiometric $[Ca^{2+}]_i$ measurements, and at 380 nm in the overload experiments. MagFura-2 and calcium orange-5N were excited at 380 nm and 545 nm, respectively. Excitation light was coupled to the microscope via a light guide. UV light was attenuated to 10–40% with neutral density filters. A 500-nm dichroic mirror and a 510-nm long-pass emission filter (T.I.L.L. Photonics) were usually used for measurements with Fura-2 or MagFura-2. A 560-nm dichroic and a 565–595-nm band pass (Omega Optical, Brattleboro, VT) were used for measurements with calcium orange-5N. In the Fura-2 overload experiments fluorescence was normalized to the fluorescence of beads that have an excitation maximum at 470 nm; therefore a 400-nm dichroic and a 410-nm long pass were used. Fluorescence was measured using a 12-bit, cooled charge-coupled device (CCD) camera (ATC-5; Photometrics, Tucson, AZ). An action potential evoked a fluorescence signal, the duration of which strongly depended on the affinity and the concentration of the indicator used (Fig. 1, *D–F*). This reflects the competition for Ca^{2+} between the endogenous buffers and the Ca^{2+} indicator. Three different experimental approaches were used to quantitatively measure the different aspects of the Ca^{2+} dynamics associated with a single presynaptic action potential as outlined below.

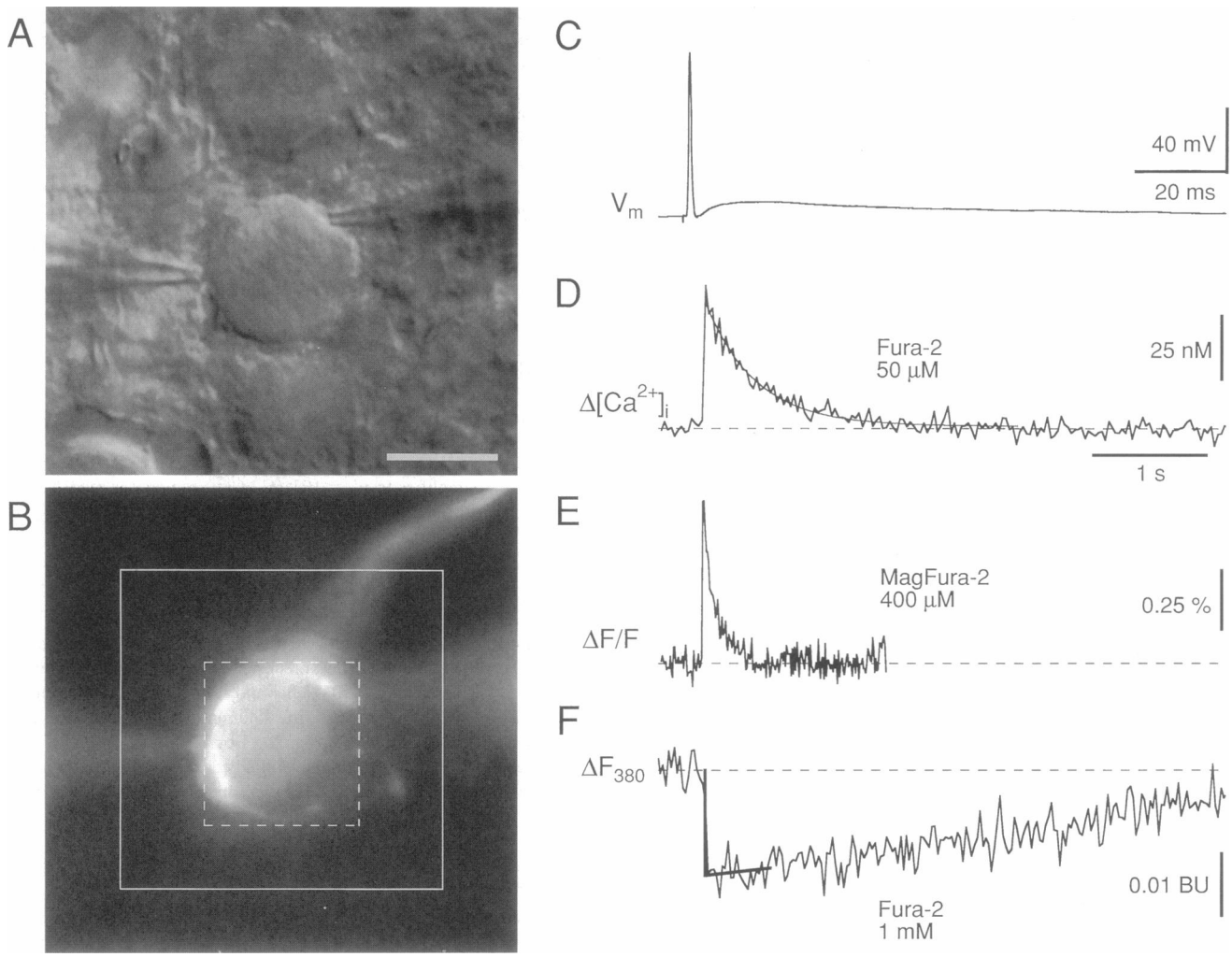

FIGURE 1 Ca^{2+} signals in the calyx of Held evoked by single action potentials. (*A*) IR-DIC video image of a MNTB principal neuron, covered by a calyx of Held, in a rat brainstem slice. The tips of two pipettes recording from the same terminal are shown. Scale bar, 10 μm. (*B*) Fluorescence image of the calyx shown in *A*, the preterminal axon (*top right*) and the two attached pipettes (containing 1 mM Fura-2). Squares indicate regions selected in different types of fluorescence measurements. For ratiometric measurements and for measurements with low-affinity indicators, regions containing the terminal but not the pipette were selected (*rectangle with dashed lines*). In the Fura-2 overload experiments, a larger region was selected (*rectangle with solid lines*). The fluorescence of one or two pipettes within this larger region did not affect the measurements, because only the changes of the absolute fluorescence intensity were evaluated. (*C*) Presynaptic action potential in a calyx of Held, followed by a depolarizing after-potential. The action potential was evoked by orthodromic stimulation. Resting membrane potential was −80 mV, temperature 23°C. (*D–F*) Presynaptic fluorescence signals evoked by single action potentials in terminals loaded with different calcium indicators. Time scale applies to *D–F* and is different from *C*. (*D*) Increase in the free calcium concentration ($\Delta[Ca^{2+}]_i$), measured ratiometrically using 50 μM Fura-2. An exponential curve is fitted to the decay of the transient (time constant 440 ms). (*E*) Relative fluorescence change $\Delta F/F$ of the low-affinity indicator MagFura-2 at 380-nm excitation (average of 20 sweeps). (*F*) Fluorescence change at 380-nm excitation (ΔF_{380}) under conditions of Fura-2 overload (1 mM). ΔF_{380} is given in bead units (BU). The fluorescence decrement was evaluated as the difference between the baseline and a regression line to the fluorescence signal in the 0.5 s after the action potential (*thicker lines*). All measurements were made at 23°C.

Ratiometric $[Ca^{2+}]_i$ measurements

Fura-2 measurements of $[Ca^{2+}]_i$ were done using 357/385 nm ratioing at 33–40 Hz (Fig. 1 *D*). Each frame transfer on the CCD chip was synchronized with a change in the excitation wavelength. The average fluorescence from a region containing a terminal but no pipette (Fig. 1 *B*, *broken square*) was measured by binning the pixels on the CCD chip. Background fluorescence was measured directly before and after each sweep from an adjacent region, interpolated linearily, and subtracted (Helmchen et al., 1996). Small fluorescence offsets between the terminal and the background region, observed before break-in, were corrected. Single exponentials were fitted to the decays of the $[Ca^{2+}]_i$ transients with a fit range that started one point after the peak and extended to three times the time interval to decay to 10% of the peak change. The amplitude of the $[Ca^{2+}]_i$ transients is given as the value of the exponential fit at the moment of the action potential.

Fluorescence signals were converted to $[Ca^{2+}]_i$ using the standard ratioing equation (Grynkiewicz et al., 1985). Calibration parameters were obtained from in vivo calibrations. R_{min} and the effective binding constant K_{eff} were determined by loading at least three terminals at each temperature with the intracellular solution containing 20 mM EGTA and 13.3 mM CaEGTA plus 6.7 mM EGTA, respectively (the dissociation constant of EGTA was assumed to be 145 nM and 119 nM at 23°C and 35°C, respectively; Groden et al., 1991). At the end of four experiments at 23°C

and six experiments at 35°C, R_{max} was determined by stimulating the terminals for up to 4 s at 100 Hz, which led to saturation of the Fura-2 response. The dissociation constant (K_d) of Fura-2, calculated as $K_d = K_{eff}(R_{min}/R_{max})$ (Neher and Augustine, 1992), was 273 and 263 nM at 23°C and 35°C, respectively.

Ca^{2+} signals measured using low-affinity indicators

Fluorescence signals of MagFura-2 and calcium orange-5N were measured at a single excitation wavelength at a frame rate of 100 Hz (e.g., Fig. 1 *E*). The selected terminal regions were similar to those used for ratiometric measurements. Background-subtracted signals are expressed as relative fluorescence changes from prestimulus levels ($\Delta F/F$). Single action potentials evoked changes of only 1% or less; therefore 20–50 sweeps were typically averaged to obtain a sufficient signal-to-noise ratio. The K_d values of MagFura-2 and calcium orange-5N were assumed to be 45 μM (Konishi and Berlin, 1993) and 20 μM (Molecular Probes catalog), respectively, which are based on in vitro measurements. We did not try to determine the K_d values in vivo. The K_d values may be twice as high in cytoplasm than in vitro (Zhao et al., 1996), but this would change our estimate of the endogenous Ca^{2+}-binding ratio in Fig. 3 *B* only from 20 to 35. For MagFura-2, $\Delta F/F$ was also converted to absolute $[Ca^{2+}]_i$ values using the formula (Jaffe et al., 1992)

$$[Ca^{2+}]_i = \frac{[Ca^{2+}]_{rest} + K_d(\Delta F/F)/(\Delta F/F)_{max}}{(1-(\Delta F/F)/(\Delta F/F)_{max})}, \quad (4)$$

where $(\Delta F/F)_{max}$ is the maximum fluorescence change upon saturation. The fluorescence intensity of MagFura-2 at 380-nm excitation decreases with increasing $[Ca^{2+}]_i$; therefore $(\Delta F/F)_{max}$ cannot exceed 100%. At the end of three experiments with MagFura-2, terminals were stimulated for 8 s at 100–200 Hz, which led to membrane depolarization, massive Ca^{2+} influx, and fluorescence changes up to 74–80%. We assume that this is close to the maximum fluorescence change and used 78% for $(\Delta F/F)_{max}$. For small $\Delta F/F$ values ($(\Delta F/F) \ll (\Delta F/F)_{max}$), as is the case for an action potential, Eq. 4 simplifies to a linear relationship between the increase in $[Ca^{2+}]_i$ and $\Delta F/F$:

$$\Delta[Ca^{2+}]_i = [Ca^{2+}]_i - [Ca^{2+}]_{rest} = \frac{K_d}{(\Delta F/F)_{max}}(\Delta F/F). \quad (5)$$

Fura-2 overload

Fura-2 (1 mM) was used to overload terminals and to measure the total Ca^{2+} influx per action potential (Fig. 1 *F*). The decrement in absolute Fura-2 fluorescence (ΔF_{380}) evoked by a Ca^{2+} influx depends on the relative amount of the exogenous and the endogenous Ca^{2+}-binding ratio (Neher, 1995):

$$\Delta F_{380} = \Delta F_{max}\frac{\kappa'_B}{(1 + \kappa_S + \kappa'_B)}. \quad (6)$$

In the case of dye overload ($\kappa'_B \gg \kappa_S$) the decrement approaches the maximum value ΔF_{max}, which is directly proportional to the total Ca^{2+} influx:

$$\Delta F_{380} = \Delta F_{max} = f_{max} Q_{Ca} \quad (\kappa'_B \gg \kappa_S). \quad (7)$$

Fluorescence decrements were evaluated as the difference (at the moment of the action potential) of the regression lines to 0.5 s before and after the fluorescence step (Fig. 1 *F*). The proportionality constant f_{max} (also termed maximum *F/Q* ratio; Schneggenburger et al., 1993) was determined by measuring fluorescence decrements evoked by Ca^{2+} currents in the presence of Na^+ and K^+ channel blockers. To account for changes in the illumination intensity or the detection efficiency in the course of these experiments, ΔF_{380} was normalized to the fluorescence of beads (4.5-μm-diameter fluoresbrite BB beads, lot 460565; Polysciences, Warrington, PA) and expressed in "bead units" (BU) (Schneggenburger et al., 1993). The bead unit was measured on each experimental day as the mean fluorescence of five beads at 380-nm excitation. Fluorescence signals were measured on a fixed region of the CCD chip, corresponding to a region of 31 × 31 μm^2 (Fig. 1 *B*, *solid square*). We chose a large fixed region and focused on the center of the synapse to ensure that all terminal fluorescence was captured. Control measurements in which the focal plane was varied showed that even with complete defocusing ($\Delta z = 30$ μm), ΔF_{380} still was 60–70% of the in-focus value.

3D image reconstruction

Fluorescence images were taken at different focal planes ($\Delta z = 0.85$ μm) with 0.5- to 1-s exposure time, using the additional twofold magnification (resulting pixel size, 0.17 μm) and a piezoelectric focusing device attached to the objective (PIFOC P-721.10; Physik Instrumente, Waldbronn, Germany). The three-dimensional image was deblurred in Fourier space with a simple inverse filtering approach (Agard et al., 1989):

$$F = G\frac{OTF}{OTF^2 + \alpha}. \quad (8)$$

G and *F* are the 3D Fourier transforms of the raw image and the deblurred image, respectively, and *OTF* is the 3D optical transfer function of the microscope. A theoretical approximation was used for the *OTF* (Erhardt et al., 1984), and the restoration parameter α was set to 0.001.

Estimate of accessible volume

The volume (*V*) of the nerve terminal accessible to Ca^{2+} was determined in two different ways. First, *V* was calculated by using the time constant of Fura-2 loading (τ_L) and the pipette series resistance (R_S) according to the equation given in Oliva et al. (1988):

$$V = \frac{\tau_L \rho D_{Fura\text{-}2}}{R_S}. \quad (9)$$

A value of 166 $\mu m^2 \cdot s^{-1}$ was used for the diffusion coefficient of Fura-2 $D_{Fura\text{-}2}$ (Adler et al., 1991) and 70 $\Omega \cdot$ cm for the specific resistance ρ of the pipette solution. The values obtained from Eq. 9 may not be accurate, because it neglects the diffusional sink of the preterminal axon and because of the uncertainty in the values for the diffusion constant of Fura-2 and the cytoplasmic resistivity. Alternatively, *V* was calculated using an equation given in Neher and Augustine (1992):

$$V = \frac{Q_{Ca} F_{357}}{2F[B]_T}\frac{(R_{min}^{-1} - R_{max}^{-1})}{\Delta F_{max}}, \quad (10)$$

where F_{357} is the isosbestic absolute fluorescence intensity after full loading with Fura-2. In addition, an estimate of the total terminal volume was obtained from the reconstructed terminals, as described in the legend of Fig. 6.

RESULTS

Loading of nerve terminals with Ca^{2+} indicators

Presynaptic terminals (calyces of Held) in the medial nucleus of the trapezoid body (MNTB) in rat brainstem slices were visualized using IR-DIC video microscopy and loaded with fluorescent Ca^{2+} indicators via whole-cell patch pi-

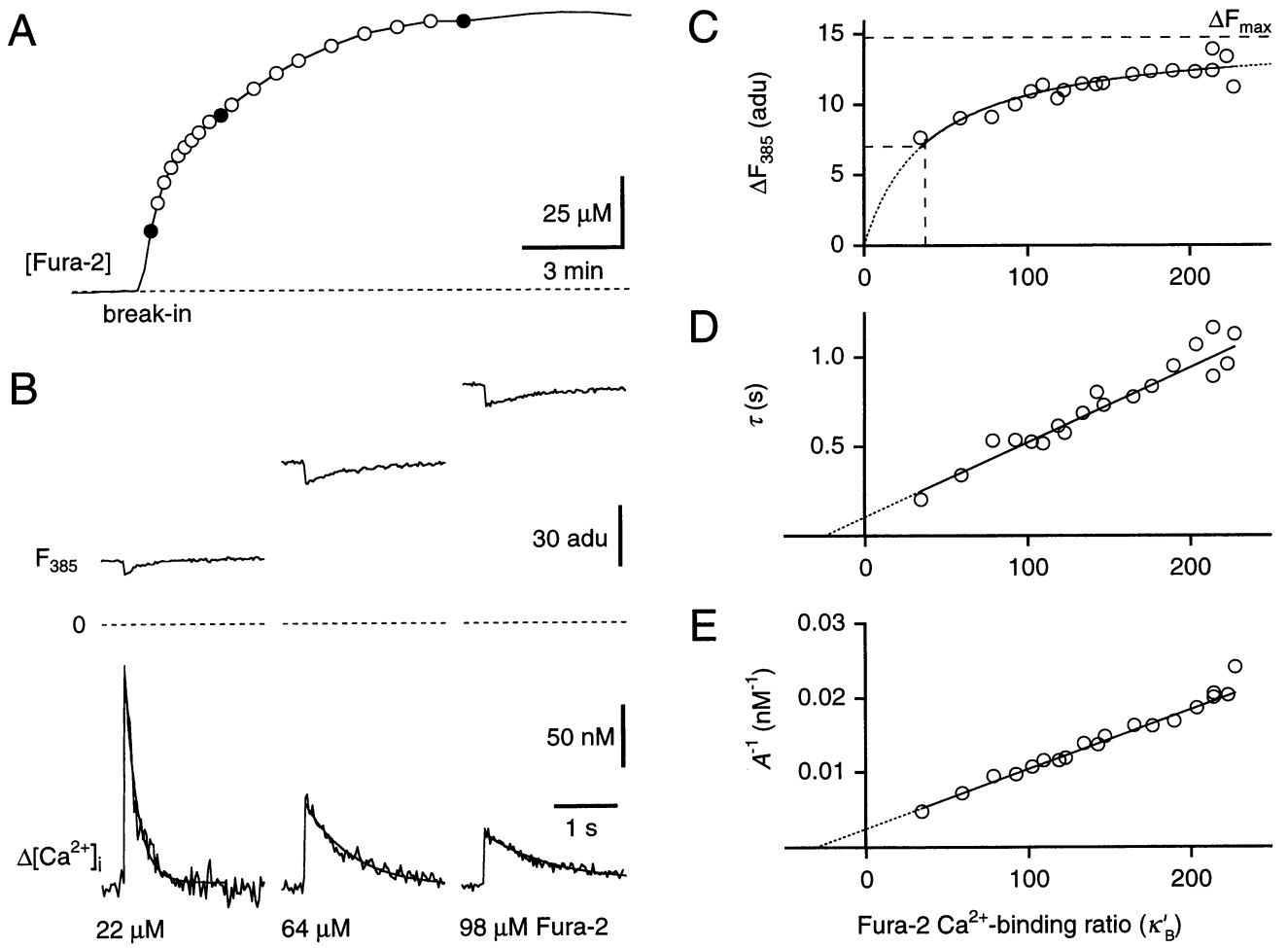

FIGURE 2 $[Ca^{2+}]_i$ transients during Fura-2 loading. (*A*) Loading of a presynaptic terminal with 100 μM Fura-2 was monitored using the fluorescence at the isosbestic excitation wavelength (*line*). $[Ca^{2+}]_i$ transients evoked by single action potentials were measured at 12–60-s intervals during Fura-2 loading (indicated by *circles*). (*B*) Fluorescence signals at 385-nm excitation (F_{385}) and the corresponding transients after conversion to $[Ca^{2+}]_i$, measured directly after break-in, during Fura-2 loading and after complete loading (*filled circles* in *A*). Absolute fluorescence is expressed in analog-to-digital units (adu) of the CCD camera. Fluorescence changes ΔF_{385} were evaluated as the difference between the prestimulus fluorescence level and a regression line fitted to six to eight data points after the maximum fluorescence decrease. Exponential curves were fitted to the decays of the $[Ca^{2+}]_i$ transients with time constants of 0.20, 0.80, and 1.13 s, respectively. (*C–E*) Absolute fluorescence decrement ΔF_{385}, decay time constant τ, and inverse of the peak amplitude A^{-1} as a function of the Fura-2 Ca^{2+}-binding ratio κ'_B. The smooth curve in *C* is a fit according to Eq. 6, with ΔF_{max} and κ_S as free parameters ($\kappa_S = 37$). Regression lines through the first eight points of the τ and the A^{-1} plots yielded extrapolated *y* axis intercepts corresponding to 0.104 s and 404 nM for time constant and amplitude at $\kappa'_B = 0$ (regression coefficients *r* of 0.93 and 0.99, respectively). Negative *x* axis intercepts were 25 and 31, respectively. All data are from the same experiment at 23°C.

pettes (Fig. 1, *A* and *B*). The structure of the terminals was similar to the published descriptions of the calyx of Held at this developmental stage, with finger-like extensions of the preterminal axon covering large parts of the principal neuron (see also Fig. 6; Morest, 1968; Forsythe, 1994; Borst et al., 1995). Single presynaptic action potentials were evoked by orthodromic stimulation (Fig. 1 *C*), and the fluorescence of the Ca^{2+} indicator was measured with a CCD camera (Fig. 1, *D–F*). We used three different experimental approaches, examples of which are shown in Fig. 1, *D–F*, and which are described in detail in Materials and Methods, to quantitatively study presynaptic calcium dynamics in individual nerve terminals.

Presynaptic $[Ca^{2+}]_i$ transients strongly depend on Fura-2 concentration

The high-affinity indicator Fura-2 was used to determine the effect of an added Ca^{2+} buffer on the $[Ca^{2+}]_i$ transients and to estimate the endogenous Ca^{2+}-binding ratio of the terminals. We studied how size and duration of presynaptic $[Ca^{2+}]_i$ transients depended on the exogenous Ca^{2+}-binding ratio by measuring transients during loading with an intermediate concentration of Fura-2 (100 μM at 23°C; 160 μM at 35°C). A terminal region not containing the pipette and a background region were selected based on the IR-DIC image, when the pipette was still in the cell-attached recording

configuration. After break-in, every 12–60 s a single action potential was elicited in current clamp by orthodromic stimulation. At the same time Fura-2 fluorescence signals were measured at 357- and 385-nm excitation. The Ca^{2+}-insensitive fluorescence (F_{357}) was used to monitor the diffusion of Fura-2 into the terminal. We assumed that the concentration of the indicator dye in the terminal was equal to the concentration in the pipette when F_{357} reached a plateau level (Fig. 2 *A*). Indicator dye loading followed an approximately exponential time course, and was complete within 5–10 min with series resistances of the loading pipette of 20–30 MΩ. The Fura-2 concentrations were used to calculate the Ca^{2+}-binding ratio of Fura-2 (κ'_B) at the moment of each measurement (Eq. 1). Resting calcium concentrations were around 40 nM.

The decrement of the fluorescence intensity at 385-nm excitation (ΔF_{385}) that was evoked by a single action potential increased during Fura-2 loading (Fig. 2 *B*, *upper traces*). At full loading with 100 μM Fura-2 (corresponding to a κ'_B of about 230), ΔF_{385} already approached the maximum value ΔF_{max}, as seen from the fit of Eq. 6 to the plot of ΔF_{385} versus Fura-2 Ca^{2+}-binding ratio κ'_B (Fig. 2 *C*). The half-maximum value of ΔF_{385} provides an estimate of the endogenous Ca^{2+}-binding ratio κ_S and was on average 44 ± 6 at 23°C (n = 8, mean ± SEM). This means that the addition of about 25 μM Fura-2 doubles the Ca^{2+}-binding capacity of the terminal. The fluorescence signals were ratiometrically converted to $[Ca^{2+}]_i$. The $[Ca^{2+}]_i$ transients progressively decreased in amplitude during Fura-2 loading, and their time course was prolonged (Fig. 2 *B*, *lower traces*). The dependencies of the decay time constant (τ) and of the inverse of the amplitude (A^{-1}) on κ'_B were both well described by a linear relationship according to Eq. 3 (Fig. 2, *D* and *E*). Extrapolation to $\kappa'_B = 0$ yielded 407 ± 90 nM and 91 ± 13 ms as estimates of the amplitude and the time constant of the Ca^{2+} signal in the absence of exogenous buffers (n = 8; 23°C). At 35°C, amplitudes of the transients were similar, but the decays were faster (see below Table 1). The negative x axis intercepts of the plots of τ and A^{-1} versus κ'_B provide another estimate of the Ca^{2+}-binding ratio κ_S of the endogenous buffer (Neher and Augustine, 1992; Helmchen et al., 1996). Average κ_S values obtained by this method were between 26 and 71 with a mean of about 40. Thus, about 2.5% of the calcium ions entering the presynaptic terminal during an action potential remain free.

Low-affinity indicators reveal large and fast presynaptic $[Ca^{2+}]_i$ transients

As shown in Fig. 2, a high-affinity Ca^{2+} indicator such as Fura-2 alters the presynaptic $[Ca^{2+}]_i$ transients. Indicators with a lower affinity increase the Ca^{2+}-binding capacity of the terminal only a little and for this reason are expected to affect $[Ca^{2+}]_i$ transients much less. Therefore, we measured $[Ca^{2+}]_i$ transients with the low-affinity indicators MagFura-2 and calcium orange-5N, and compared their size and time course with the results obtained with Fura-2 by extrapolating to zero concentration of Fura-2.

Single action potentials evoked relative fluorescence changes of the low-affinity indicators of only 1% or less (Fig. 3 *A*). Therefore, after 10 min of dye loading, 20–30 (in a few cases 50–100) sweeps were acquired in 30-s intervals and averaged. The signals measured with 400 μM MagFura-2 reached peak values within two sample points (i.e., within 20 ms) and decayed back to resting levels with time constants of 106 ± 6 ms and 45 ± 3 at 23°C and 35°C, respectively (Fig. 3 *A*, *left traces*). MagFura-2 signals were converted to $\Delta[Ca^{2+}]_i$ using Eq. 5. Peak amplitudes of the transients were on average 400–500 nM. The results of the experiments with Fura-2 and MagFura-2 agree well (see below Table 1). Transients with the amplitudes and time constants obtained by extrapolation to zero Fura-2 concentration superimpose well on the transients measured with 400 μM MagFura-2 (Fig. 3 *A*). If the endogenous Ca^{2+}-binding ratio is as low as 40 (the value estimated in the previous section), the $[Ca^{2+}]_i$ transient is expected to depend on the concentration of the low-affinity dye as well. Therefore, we also measured transients with 2 mM MagFura-2, corresponding to an exogenous Ca^{2+}-binding ratio of about 40 (Fig. 3 *A*, *middle traces*). Indeed, the transients were both reduced in size and prolonged by a factor of 2.2 compared to those measured with 400 μM. Action potentials evoked fluorescence signals of calcium orange-5N with similar time courses. This demonstrates that the MagFura-2 signals were caused by changes in the Ca^{2+} concentration and not in the Mg^{2+} concentration, because, in contrast to MagFura-2, calcium orange-5N fluorescence is not sensitive to Mg^{2+}. The decays of the transients measured with 400 μM calcium orange-5N were slightly slower than those measured with 400 μM MagFura-2 (Fig. 3 *A*, *right traces*). In Fig. 3 *B* the decay time constants, measured with different dyes at different concentrations, are plotted versus the exogenous Ca^{2+}-binding ratio. From the negative x axis intercepts an endogenous Ca^{2+}-binding ratio of about 20 is obtained. In conclusion, the low-affinity dyes and Fura-2 yielded similar estimates for the size and the time course of the $[Ca^{2+}]_i$ transients in the absence of exogenous buffers, as well as for the endogenous Ca^{2+}-binding capacity.

Using Fura-2 overload to measure the total Ca^{2+} influx per action potential

As demonstrated above, Fura-2 distorts the presynaptic $[Ca^{2+}]_i$ transients because of its high affinity for Ca^{2+}. On the other hand, this property can be used to measure the number of calcium ions entering the terminal during an action potential. If the endogenous Ca^{2+}-binding ratio κ_S of the terminal is known, a Fura-2 concentration can be chosen to overload it ($\kappa'_B \gg \kappa_S$). Assuming a resting Ca^{2+} concentration of 40 nM, 1 mM Fura-2 corresponds to a κ'_B of about 2600, considerably larger than the value of 40 estimated for κ_S. Hence at this concentration Fura-2 outcom-

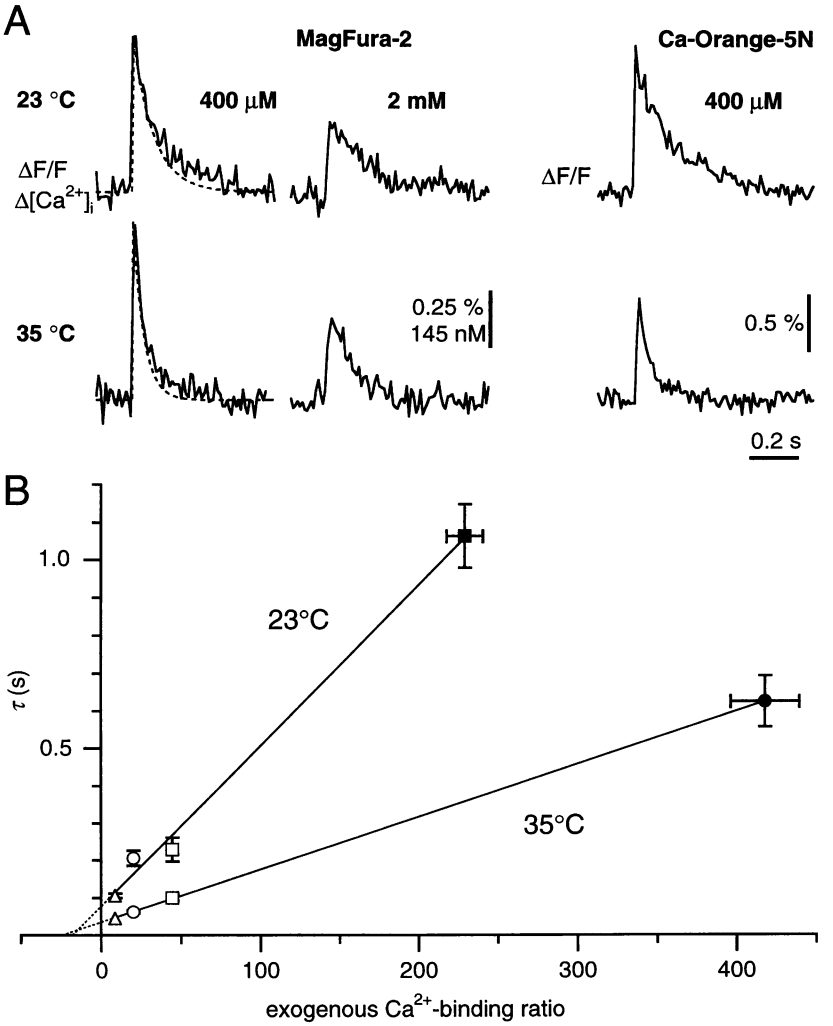

FIGURE 3 Ca^{2+} signals measured with low-affinity Ca^{2+} indicators. (*A*) Fluorescence signals evoked by single action potentials in presynaptic terminals loaded with 400 μM or 2 mM MagFura-2, or with 400 μM calcium orange-5N. Each trace is an average of 20–80 sweeps taken at a frame rate of 100 Hz. Upper traces were measured at 23°C, lower traces at 35°C. Signals are expressed as percentage changes of the fluorescence $\Delta F/F$. MagFura-2 signals were also converted to changes in calcium concentration ($\Delta[Ca^{2+}]_i$) using Eq. 5. Dashed curves represent exponential $[Ca^{2+}]_i$ transients for $\kappa'_B = 0$ using the amplitudes and time constants obtained by extrapolating to zero Fura-2 concentration (see Table 1). (*B*) Summary plot of presynaptic Ca^{2+} transient kinetics. The decay time constant τ of the transients was measured at 23°C or at 35°C, using either 100 μM Fura-2 (*filled square*), 160 μM Fura-2 (*filled circle*), 400 μM MagFura-2 (*open triangles*), 400 μM calcium orange-5N (*open circles*), or 2 mM MagFura-2 (*open squares*). The values for Fura-2 were taken from the loading experiments after complete loading. Time constants are plotted versus the exogenous Ca^{2+}-binding ratio, i.e., the Ca^{2+}-binding ratio of the indicators. For the low-affinity indicators the Ca^{2+}-binding ratio was approximated by $[B]_T/K_d$.

petes the endogenous buffers, and virtually all calcium ions that enter the terminal bind to Fura-2.

According to Eq. 7, under these conditions the fluorescence decrement at 380-nm excitation (ΔF_{380}) is proportional to the total Ca^{2+} charge (Q_{Ca}). To determine the proportionality constant f_{max} between ΔF_{380} and Q_{Ca} we measured fluorescence decrements that were evoked by pharmacologically isolated presynaptic Ca^{2+} currents (Fig. 4). Ca^{2+} currents were evoked by 10-ms voltage steps to different potentials (Fig. 4 *A*). To check the accuracy of the voltage clamp, the membrane potential was monitored with a second pipette in current-clamp mode (Borst et al., 1995). Ca^{2+} currents activated around −40 mV and had peak amplitudes of 1.5–2 nA at around 0 mV. Simultaneously measured fluorescence decrements were large and depended on the membrane potential as well (Fig. 4 *B*). Fig. 4 *C* shows the voltage dependence of ΔF_{380} and of Q_{Ca}, which was obtained by integrating the Ca^{2+} currents. Both curves superimpose, and f_{max} was determined as the slope of the plot of ΔF_{380} versus Q_{Ca} (Fig. 4 *C*, *inset*). In three experiments with maximum voltage escapes of less than 10 mV, f_{max} was 15 ± 0.5 BU · nC^{-1}. In an additional four experiments with maximum voltage escapes larger than 10 mV, f_{max} was between 13.2 and 16.4 BU · nC^{-1}. A different protocol, in which voltage steps to 0 mV with progressively increasing pulse durations were given, yielded similar values for f_{max} (data not shown).

Knowing f_{max}, we quantified the total Ca^{2+} influx per action potential in normal extracellular solution. In terminals loaded with 1 mM Fura-2, single action potentials evoked fluorescence signals consisting of an initial decrement followed by a slow recovery (Fig. 1 *F*). The ΔF_{380} values were converted to Ca^{2+} charge according to Eq. 7. On average the charge carried by calcium ions was 0.96 ± 0.06 pC at 23°C (n = 14) and 0.82 ± 0.05 pC at 35°C (n = 6). This means that 2.5–3 × 10^6 calcium ions (about 4–5 × 10^{-6} pmol) enter the presynaptic terminal during an action potential. According to our estimate of the endogenous Ca^{2+}-binding ratio, 2.5% of this number, i.e., 6–8 × 10^4 calcium ions, remain free.

Dependence of presynaptic Ca^{2+} influx on external calcium

Because the total Ca^{2+} influx per action potential could be quantified, the modulation of presynaptic Ca^{2+} influx was

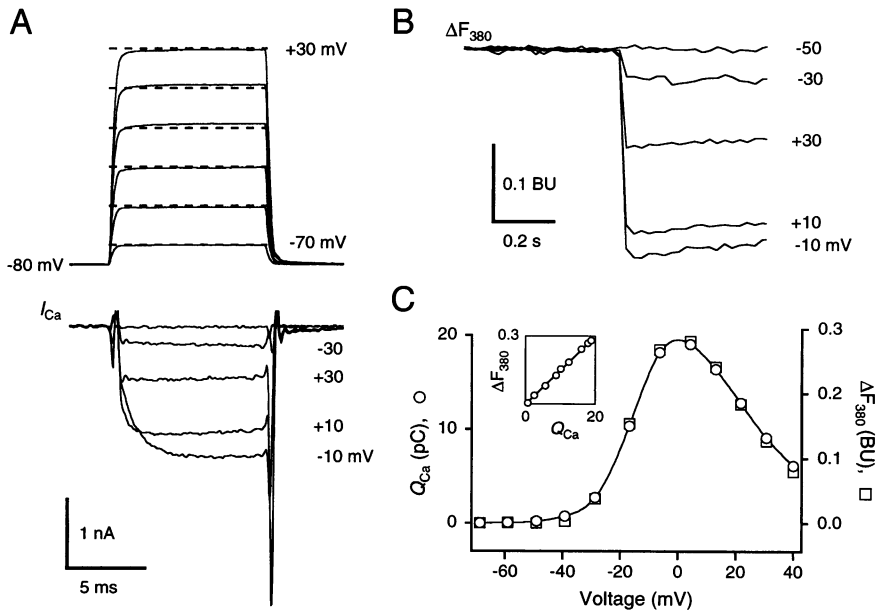

FIGURE 4 Determination of f_{max} using voltage clamp of presynaptic Ca^{2+} currents. (*A*) Voltage clamp of a terminal to different command potentials at 10 mV increments from a holding potential of −80 mV. (*Upper traces*) Membrane voltage measured with a separate pipette. Dashed lines are command voltages. (*Lower traces*) Ca^{2+} current (I_{Ca}) recordings. Numbers on the right indicate command voltages. Every second voltage and current record is shown. The passive current response to the step to −70 mV was used to correct for leak and capacitive currents after appropriate scaling. (*B*) Simultaneously measured absolute fluorescence changes at 380-nm excitation (ΔF_{380}) with 1 mM of Fura-2 in the terminal. Numbers on the right indicate command voltages. (*C*) Charge Q_{Ca} (*open circles*) and fluorescence decrement ΔF_{380} (*open squares*) as a function of membrane potential. Q_{Ca} was obtained by integrating the current traces shown in *A*. The smooth curve is a cubic spline through the Q_{Ca} data points. The value of f_{max} was determined as the slope of the regression line of the plot of ΔF_{380} (in BU) versus Ca^{2+} charge in pC and was 15.1 BU · nC^{-1} in this experiment (*inset*; $r > 0.999$). Data are from the calyx shown in Fig. 1, *A* and *B*.

studied at the level of a single mammalian CNS synapse. We measured the dependence of presynaptic Ca^{2+} influx on the external calcium concentration $[Ca^{2+}]_o$. After a 10-min loading period with 1 mM Fura-2, fluorescence decrements ΔF_{380} were evoked every 40 s by single action potentials. $[Ca^{2+}]_o$ was lowered from 2 mM (control) to concentrations in the range of 0.25 to 1.5 mM, while $[Mg^{2+}]_o$ was adjusted to keep the total extracellular divalent concentration constant. In the experiment shown in Fig. 5, ΔF_{380} was 0.0135 BU in 2 mM $[Ca^{2+}]_o$ (Q_{Ca} = 0.91 pC). Reduction of $[Ca^{2+}]_o$ to 1 and 0.25 mM reduced ΔF_{380} to 63 and 18%, respectively (Fig. 5, *A* and *B*). Q_{Ca} returned to the control value after switching back to 2 mM $[Ca^{2+}]_o$, even after almost 1 h of whole-cell recording. This was regularly observed, except in one experiment in which Q_{Ca} had increased to 140% of its initial value after 50 min. Fig. 5 *C* shows the relationship between Q_{Ca} and $[Ca^{2+}]_o$ as obtained from 14 experiments. It is nearly linear for low external Ca^{2+} concentrations and shows some saturation of Q_{Ca} at higher concentrations. Saturation of presynaptic Ca^{2+} influx with increasing $[Ca^{2+}]_o$ has been attributed to the binding of permeating calcium ions to the pore of the calcium channels and can be described by a bimolecular binding process (Augustine and Charlton, 1986). Thus, with the method of Fura-2 overload the modulation of action potential-evoked Ca^{2+} influx in individual CNS nerve terminals can be studied.

Volume estimate of the presynaptic terminal

To correlate the number of calcium ions flowing into the presynaptic terminal with the measurements of free Ca^{2+} concentration, we obtained several estimates of the terminal volume. The total volume of the terminals was estimated from nine stacks of fluorescence images that were acquired after retraction of the pipette (Fig. 6 *A*). Terminals were reconstructed by deblurring the three-dimensional image, and a threshold gray level was set to obtain an estimate of the total terminal volume, yielding a range of 350–1050 μm^3 (Fig. 6, *B* and *C*). This estimate, however, is rough and may include volume not accessible to Ca^{2+}.

The volume accessible to Ca^{2+} (V) was determined using Eqs. 9 and 10 (see Materials and Methods). In a simple description of dye loading, the intraterminal dye concentration rises exponentially with a time constant τ_L, which depends on the pipette series resistance, the resistivity of the pipette solution, the diffusion constant of Fura-2, and V (Eq. 9). This assumes that the tip of the pipette forms the major diffusional barrier, which has already been shown for dye loading of the calyx (Borst et al., 1995). For the Fura-2 loading experiments, V calculated in this way was between 200 and 620 μm^3, with an average of 390 ± 53 μm^3 (n = 8). Alternatively, an equation based on the usage of the isosbestic wavelength was applied (Eq. 10). In the Fura-2 loading experiments, the relevant parameters of Eq. 10 were

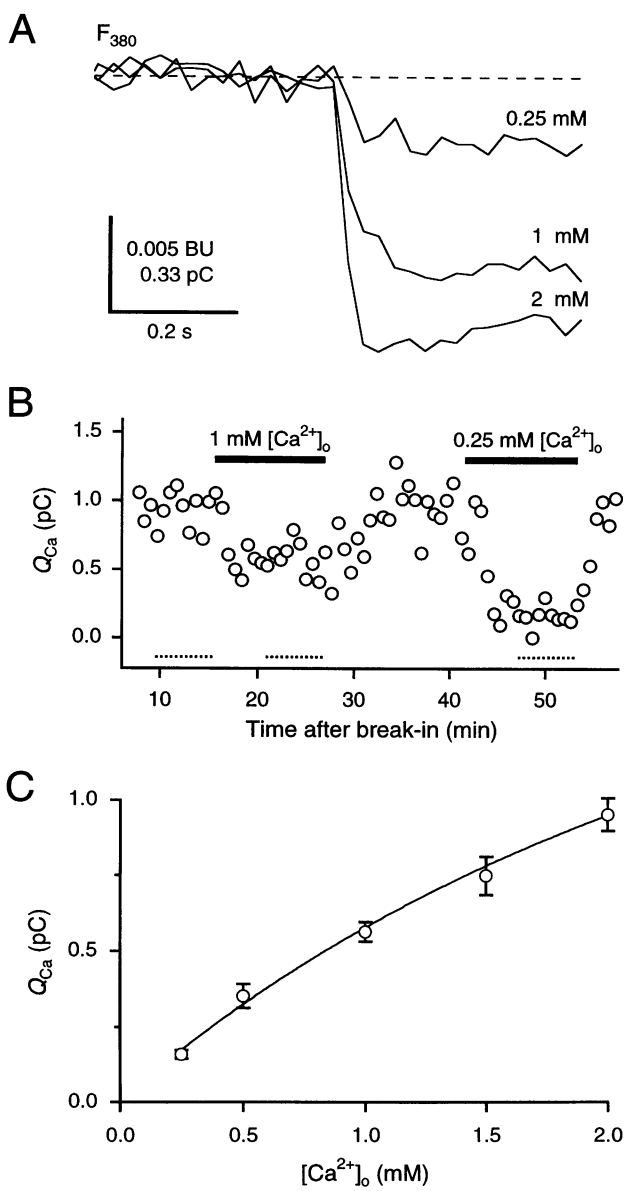

FIGURE 5 Dependence of total Ca^{2+} influx per action potential on external Ca^{2+} concentration. (*A*) Fluorescence decrements at 380-nm excitation (ΔF_{380}) with 0.25, 1, and 2 mM external Ca^{2+} concentration ($[Ca^{2+}]_o$) measured in a presynaptic terminal that was filled with 1 mM Fura-2. Each trace is an average of nine sweeps. Decrements were expressed in bead units (BU) and converted to Ca^{2+} charge (Q_{Ca}) using f_{max} (scale bar in pC). (*B*) Time course of Q_{Ca} during the experiment. Single action potentials were evoked at 40-s intervals, and $[Ca^{2+}]_o$ was lowered from 2 mM (*control*) to 1 and 0.25 mM during two periods, each lasting 10 min. The sweeps measured during the periods indicated by the dotted lines were averaged to obtain the traces shown in *A*. (*C*) Summary plot showing the dependence of Q_{Ca} on $[Ca^{2+}]_o$. Data are shown as mean ± SEM (n = 4–6). The data are well described by a bimolecular binding reaction with a dissociation constant of 3.6 mM (*solid line*).

either measured or known from calibration experiments. Using the derived values for ΔF_{max} (Fig. 2 *C*) and a value of 0.96 pC for Q_{Ca}, V was in the range of 170–570 μm^3, with an average of 390 ± 50 μm^3 (n = 8, 23°C). Thus Eqs. 9 and 10 both yield an estimate for V of about 400 μm^3 (0.4 pl). This also agrees reasonably well with the rough estimate for the total terminal volume. In addition, it is consistent with the estimates of the free Ca^{2+} concentration change and of the endogenous Ca^{2+}-binding ratio. This can be seen by dividing the number of calcium ions entering the terminal ($4–5 \times 10^{-6}$ pmol) by 0.4 pl, which yields 10–13 μM for the average total Ca^{2+} concentration change in the terminal. Taking into account that about 2.5% of the calcium ions remain free, this is in reasonable agreement with the measured increase in the free Ca^{2+} concentration of about 400 nM.

Table 1 and Fig. 7 summarize the results obtained for the Ca^{2+} dynamics associated with a single action potential in the calyx of Held. Values for all aspects according to the single compartment model are given. The Ca^{2+}-binding ratio was obtained from the plots of A^{-1}, τ, or ΔF_{385} versus the Fura-2 Ca^{2+}-binding ratio κ'_B. Amplitude and decay time constant of the $[Ca^{2+}]_i$ transient, nearly unaffected by exogenous buffers, were determined either by extrapolation of the Fura-2 loading experiments or by direct measurement using MagFura-2.

DISCUSSION

The following picture of Ca^{2+} dynamics associated with a single action potential in the calyx of Held arises. During an action potential $4–5 \times 10^{-6}$ pmol of calcium ions enter the terminal, which has an accessible volume of about 0.4 pl. This causes an increase in the total concentration of calcium (free and bound) by 10–13 μM. With an endogenous Ca^{2+}-binding ratio of about 40, 2.5% of the inflowing calcium remains free, yielding 300–400 nM for the increase in cytoplasmic $[Ca^{2+}]_i$. The removal of free Ca^{2+} is rapid, with a rate of up to 900 s^{-1} at physiological temperatures. This means that after an action potential $[Ca^{2+}]_i$ returns to the resting level after 100 ms (Fig. 7). The independent measurements of Ca^{2+} influx, volume, and Ca^{2+} concentration and the values for the Ca^{2+}-binding ratio and for the size and duration of the $[Ca^{2+}]_i$ transients (determined by low- and high-affinity indicator measurements) are consistent with this picture of Ca^{2+} influx, buffering, and extrusion (Table 1).

Influx

Direct measurements of the presynaptic Ca^{2+} current at the squid giant synapse and at the rat MNTB synapse have shown that inflow occurs during the repolarization phase of the action potential and lasts less than 1 ms (Llinás et al., 1982; Borst and Sakmann, 1996). In these studies Ca^{2+} currents were pharmacologically isolated and were evoked by action potential waveform voltage-clamp commands. We extended the method of Fura-2 overload, which previously has been used to determine fractional Ca^{2+} currents through ligand-gated ion channels (for a review see Neher, 1995), to the measurement of the time integral of the Ca^{2+}

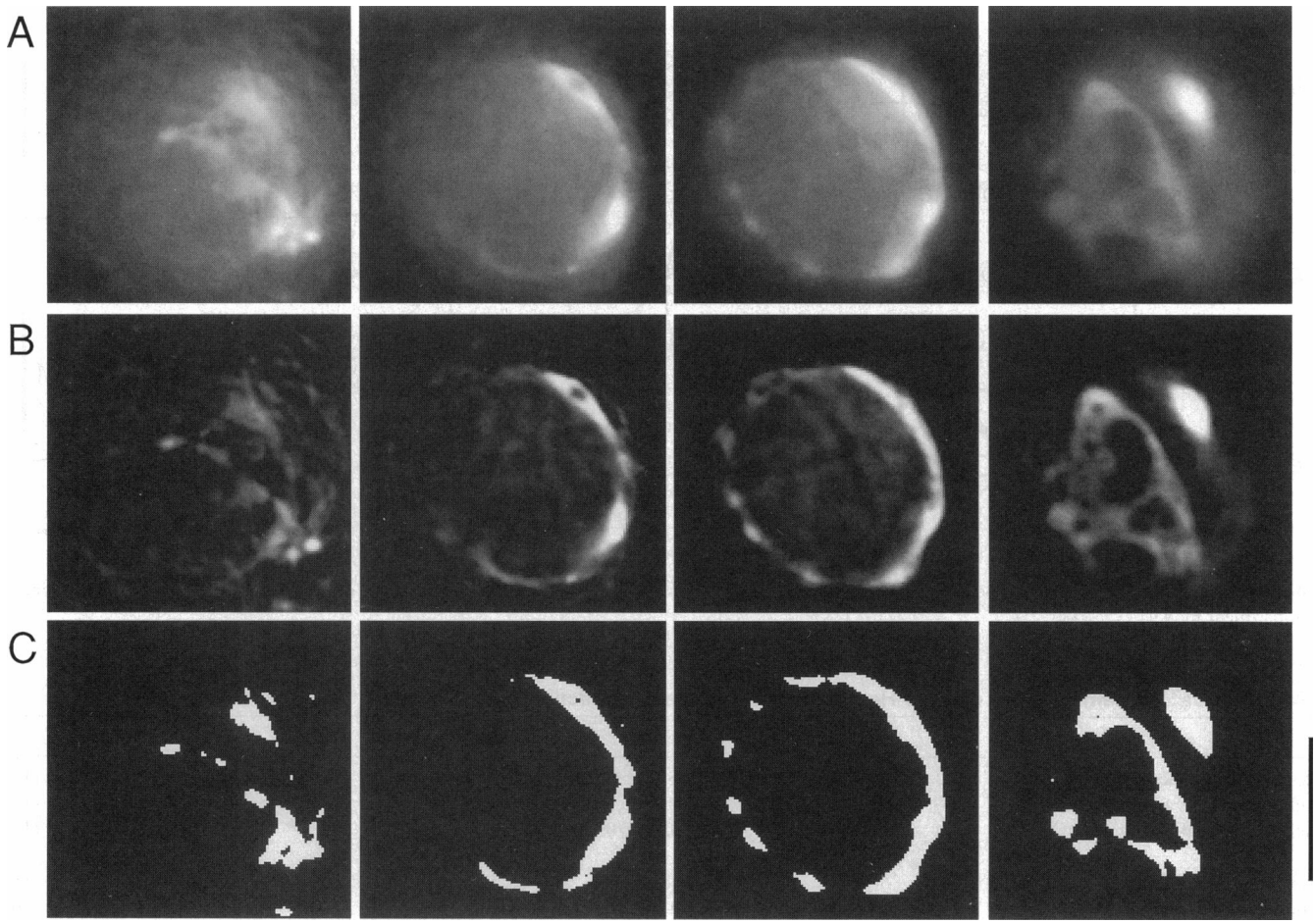

FIGURE 6 Volume estimate of a calyx of Held from a 3D reconstruction. (*A*) Fluorescence images of a calyx of Held loaded with 400 μM MagFura-2, taken at different focal planes after retraction of the patch pipette. From left to right, the focal plane changes from above to below the principal neuron. The preterminal axon entering the slice is seen in the rightmost images in the upper right corner. (*B*) Deblurred images after applying a 3D restoration filter to the stack of fluorescence images. (*C*) Binary images obtained by a threshold segmentation of the deblurred images shown in *B*. The threshold gray value was set to 3 times the gray level in the center of the middle section after deblurring (the position of the unstained principal neuron), and volume elements with gray values above the threshold were assigned to the terminal. Scale bar, 10 μm.

current during an action potential (Q_{Ca}) in normal extracellular solution. The value of 0.96 pC for Q_{Ca} that we obtained at 23°C agrees well with the time integral of the presynaptic Ca^{2+} current at the calyx of Held (0.89 pC; Borst and Sakmann, 1996). This charge corresponds to 1.4×10^4 calcium ions entering the terminal per vesicle released, assuming a quantal content of 210 at the MNTB synapse (Borst and Sakmann, 1996). At 35°C the value of Q_{Ca} was only slightly smaller than at 23°C, although the half-width of action potentials was about half as long. Apparently, temperature-dependent changes of Ca^{2+} channel properties compensate for the reduction in the duration of the action potential. Q_{Ca} depended slightly sublinearly on the external calcium concentration, in agreement with previous reports (Augustine and Charlton, 1986; Mintz et al., 1995; Borst and Sakmann, 1996). Measuring changes in presynaptic Ca^{2+} influx using Fura-2 overload may prove useful for pharmacological studies of the relative contribution of Ca^{2+} channel subtypes to fast transmitter release (Wu and Saggau, 1994; Mintz et al., 1995) and of the modulation of Ca^{2+} influx by presynaptic adenosine, $GABA_B$, or metabotropic glutamate receptors (Barnes-Davies and Forsythe, 1995).

Buffering

The endogenous Ca^{2+}-binding ratio (κ_S) was in the range of ~40, meaning that 97.5% of the calcium entering the terminal during an action potential is rapidly bound to endogenous Ca^{2+} buffers. Previous estimates for κ_S range from 40 in squid axoplasm (Brinley, 1978), 174 in isolated rat neurohypophysial nerve endings (Stuenkel, 1994), 600 at the crayfish neuromuscular junction (Tank et al., 1995), to >10,000 in rat synaptosomes (Martinez-Serrano et al., 1992; for review see Neher, 1995). Differences in experimental conditions are likely to contribute to this extremely large range of κ_S. For example, κ_S could depend on the size

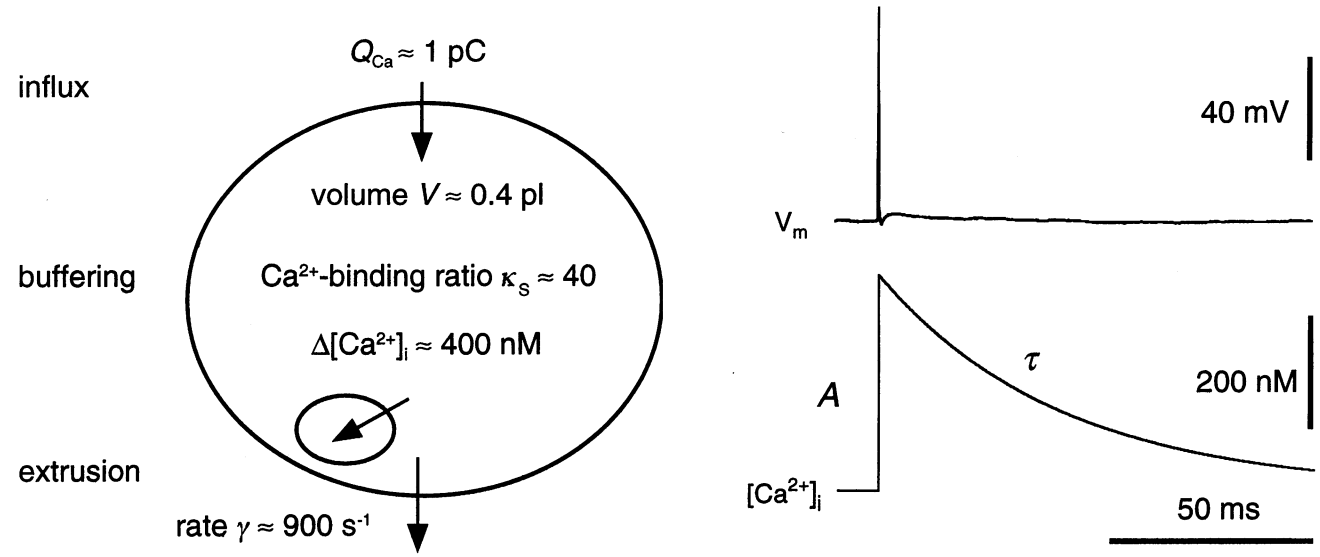

FIGURE 7 Schematic drawing of the Ca^{2+} dynamics associated with a single action potential in the calyx of Held at 35°C according to the single compartment model.

TABLE 1 Ca^{2+} dynamics in the calyx of Held associated with a single action potential

	23°C		35°C	
Resting membrane potential (mV)	−76 ± 1	(18)	−77 ± 1	(17)
Action potential amplitude (mV)	104 ± 2	(18)	94 ± 2	(17)
Action potential half-width (ms)	0.58 ± 0.03	(18)	0.26 ± 0.02	(17)
Resting $[Ca^{2+}]_i$ (nM)	46 ± 7	(8)	39 ± 7	(8)
Total Ca^{2+} influx Q_{Ca} (pC)	0.96 ± 0.06	(14)	0.82 ± 0.05	(6)
Accessible volume V (Eq. 9) (μm^3)	390 ± 53	(8)	510 ± 62	(8)
Accessible volume V (Eq. 10) (μm^3)	390 ± 50	(8)	315 ± 17	(8)
Ca^{2+}-binding ratio κ_S (from ΔF_{385})	44 ± 6	(8)	71 ± 13	(8)
Ca^{2+}-binding ratio κ_S (from τ)	26 ± 4	(8)	49 ± 23	(8)
Ca^{2+}-binding ratio κ_S (from A^{-1})	41 ± 6	(8)	37 ± 7	(8)
Amplitude* A (nM)	407 ± 90	(8)	486 ± 82	(8)
Amplitude# A (nM)	443 ± 36	(5)	507 ± 49	(3)
Decay time constant* τ (ms)	91 ± 13	(8)	47 ± 16	(8)
Decay time constant# τ (ms)	106 ± 6	(5)	45 ± 3	(3)
Ca^{2+} extrusion rate γ (s^{-1})	≈400		≈900	

* Values from extrapolation to zero Fura-2 concentration.
\# Values from terminals loaded with 400 μM MagFura-2.
All values are given as mean ± SEM (number of experiments).

of the Ca^{2+} load, being higher after larger Ca^{2+} loads (Stuenkel, 1994). On the other hand, the wide range of κ_S values may reflect differences in the content of Ca^{2+}-binding proteins. However, at present the nature of endogenous Ca^{2+} buffers is not well defined, and expression of Ca^{2+}-binding proteins is developmentally regulated (Friauf, 1993; Lohmann and Friauf, 1996).

We did not directly address the question of mobility of endogenous buffers. However, the $[Ca^{2+}]_i$ transients extrapolated from Fura-2 measurements during the first minutes after break-in agreed well with the average $[Ca^{2+}]_i$ transients measured 10–30 min after break-in with low-affinity indicators (Fig. 3 *A*). In addition, the mobile Ca^{2+} buffer BAPTA reduces postsynaptic currents at the MNTB synapse substantially when present in the terminal at a concentration of 1 mM, whereas BAPTA at 50 μM does not alter synaptic transmission measurably (Borst et al., 1995). Both observations suggest that the endogenous buffer in the calyx of Held is rather immobile, in agreement with reports on other preparations (Neher, 1995).

In the MNTB, the content of Ca^{2+}-binding proteins is different in the neuropil and in the cell bodies of principal neurons (Friauf, 1993; Lohmann and Friauf, 1996). This suggests that the Ca^{2+}-binding ratio of the pre- and postsynaptic compartments at an individual synapse could be different. The Ca^{2+}-binding ratio in the principal neurons of the MNTB has not yet been determined. However, in the proximal dendrites of neocortical and hippocampal pyrami-

dal neurons, a 2 to 4 times higher value of κ_S was found using the same method and experimental setup as described here (Helmchen et al., 1996).

Because of the relatively low endogenous Ca^{2+}-binding ratio, the $[Ca^{2+}]_i$ transients in the calyx of Held strongly depended on the amount of Ca^{2+}-binding capacity, which was added to the cytoplasm in the form of fluorescent indicators. Even an increase in the concentration of the low-affinity dye MagFura-2 from 400 μM to 2 mM reduced and prolonged the transients significantly. In contrast, Ca^{2+} transients in cerebellar granule cell terminals were not prolonged when the duration of local extracellular application of MagFura-2-AM was increased (Regehr and Atluri, 1995). A higher Ca^{2+}-binding capacity in these terminals may account for this difference, but the concentrations of the indicator were uncertain in these experiments. In a previous report we measured Ca^{2+} transients in the calyx of Held using calcium green-5N (Borst et al., 1995), which is supposed to be a low-affinity indicator (Escobar et al., 1994). However, size and duration of the transients depended on the concentration of calcium green-5N. At 200 μM the decay time constant was 0.66 s. This cannot be explained by the low endogenous Ca^{2+}-binding ratio alone. When the quantitative relationship between the time constant and the added Ca^{2+}-binding ratio is used as a lookup table (Fig. 3 *B*), 200 μM calcium green-5N should correspond to a Ca^{2+}-binding ratio of 140. This indicates that its dissociation constant was only a few μM under our conditions or that the Ca^{2+} dependence of the calcium green-5N fluorescence deviated from a one-to-one binding scheme (Ukhanov et al., 1995).

Extrusion

We used low-affinity Ca^{2+} indicators to measure the time course of the presynaptic $[Ca^{2+}]_i$ transient after a single action potential. The transient decayed with a time constant of 45 ms at 35°C. Recent studies on other CNS presynaptic terminals using MagFura-2 report a decay time constant of 150 ms in cerebellar granule cell terminals (20–23°C; Regehr and Atluri, 1995) and a half-decay time of 30 ms at the CA3-CA1 synapse (28–30°C; Sinha et al., 1997). Thus, although presynaptic terminals in the MNTB, cerebellum, and hippocampus differ greatly in size, the Ca^{2+} transients all have fast decays. This suggests rapid Ca^{2+} signaling as a general feature of CNS presynaptic terminals.

The Ca^{2+} extrusion rate (γ), calculated using Eq. 3 and assuming $\kappa_S = 40$, was 900 s^{-1} at 35°C. This means that after an increase of $[Ca^{2+}]_i$ of 400 nM evoked by an action potential, the initial velocity of the reduction in Ca^{2+} concentration is 360 nM · ms^{-1} at physiological temperatures. The extrusion rate depended on the temperature with a Q_{10} of about 2, similar to the Q_{10} reported for the decay time constant of Ca^{2+} transients in mossy fiber terminals (Regehr et al., 1994). Taking into account this Q_{10}, our estimate of γ is consistent with the value of 100 s^{-1} reported for nerve terminals at the crayfish neuromuscular junction at 8°C (Tank et al., 1995). However, the extrusion in the calyx of Held is about 40 times faster than in adrenal chromaffin cells (Neher and Augustine, 1992). This cannot be explained by a difference in surface-to-volume ratio alone. Rather, it suggests a difference in Ca^{2+} extrusion mechanisms between cellular structures in which secretion is tightly linked to the action potential, as in presynaptic terminals of the CNS or the neuromuscular junction, and others that do not display this tight coupling, e.g., chromaffin cells (Zhou and Misler, 1995). Ca^{2+} extrusion mechanisms in the calyx of Held have not yet been studied, but it seems likely that Na^+/Ca^{2+} exchange and Ca^{2+}-ATPases in the plasma membrane and in the endoplasmic reticulum contribute to the removal of cytoplasmic Ca^{2+} near resting levels, and that uptake into mitochondria may be involved after large Ca^{2+} loads (Stuenkel, 1994; Reuter and Porzig, 1995; reviewed by Blaustein, 1988).

Functional relevance

After an action potential the high concentrations of free calcium near the sites of Ca^{2+} entry rapidly collapse because of diffusion and binding (Roberts, 1994). The residual calcium, bound or free, has to be removed from the cytosol to prevent Ca^{2+} accumulation and cell damage. The initial fast reduction of localized $[Ca^{2+}]_i$ may terminate fast release if the Ca^{2+} sensor has a low affinity (Fogelson and Zucker, 1985). The remaining, residual free calcium may account for the delayed vesicle release observed in the calyx of Held (Borst and Sakmann, 1996). In addition, residual calcium controls different types of short-term enhancement of release (Zucker, 1994), and several steps in the synaptic-vesicle cycle appear to be $[Ca^{2+}]_i$ sensitive (Neher and Zucker, 1993).

The large load of free calcium ions presented to a presynaptic terminal during an action potential can be removed by buffering or by extrusion (Fogelson and Zucker, 1985). It has been suggested that presynaptic terminals contain high concentrations of cytosolic Ca^{2+}-binding sites, corresponding to a Ca^{2+}-binding ratio of more than 10,000, to cope with this Ca^{2+} load (Martinez-Serrano et al., 1992). Although such a high Ca^{2+}-binding capacity would lower $[Ca^{2+}]_i$ directly after an action potential to values near the resting level, the final decay to the resting level would take tens of seconds. As a result, Ca^{2+} would accumulate in the terminal during trains of action potentials, even at a low discharge frequency. In contrast, the MNTB presynaptic terminals have an efficient extrusion mechanism to remove Ca^{2+}, but their endogenous Ca^{2+}-binding capacity is relatively low. The functional significance of the low Ca^{2+}-binding capacity could be to minimize competition of endogenous buffers, not only with the putative Ca^{2+} receptor controlling fast release, but also with the fast extrusion mechanism. This provides an efficient way to extrude Ca^{2+} loads rapidly and to prevent accumulation of Ca^{2+} between action potentials.

APPENDIX: ASSUMPTIONS OF THE SINGLE COMPARTMENT MODEL

The single compartment model for Ca^{2+} dynamics in the calyx of Held is based on the following assumptions: 1) Ca^{2+} influx is instantaneous. 2) The Ca^{2+} extrusion mechanism is linear and nonsaturable. 3) The Ca^{2+}-binding ratios are constant. 4) Ca^{2+} is in diffusional and chemical equilibrium. Here we discuss these assumptions and find that in the case of rapid local chemical equilibration and a homogeneously distributed, nonsaturable pump, diffusional equilibrium is not a necessary assumption.

The Ca^{2+} current in the calyx of Held during an action potential recently was shown to last less than 1 ms at room temperature (Borst and Sakmann, 1996). The fluorescence signals of the low-affinity dyes reached the peak value within one or two sample points (i.e., within 10–20 ms), with no measurable deviation from an exponential decay thereafter. This indicates that Ca^{2+}-induced Ca^{2+} release does not contribute to the signal. Therefore, Ca^{2+} influx is rapid compared to the time course of the Ca^{2+} signals, validating the first assumption.

The dependence on $[Ca^{2+}]_i$ of an extrusion mechanism that follows Michaelis-Menten kinetics simplifies to a linear relationship if $[Ca^{2+}]_i$ is well below the half-maximum concentration of the pump (Tank et al., 1995). This is likely to hold in our experiments because the decay time course was well described by a single exponential. In addition, we used a small stimulus with peak volume-averaged $[Ca^{2+}]_i$ levels always below 0.8 μM. At the crayfish neuromuscular junction the time course of presynaptic $[Ca^{2+}]_i$ signals is consistent with a linear extrusion mechanism, even during trains of action potentials (Tank et al., 1995).

Ca^{2+}-binding ratios decrease with increasing $[Ca^{2+}]_i$. The estimate of the endogenous Ca^{2+}-binding ratio κ_S therefore represents a mean value if the free Ca^{2+} concentration is below 1 μM. It may change significantly for higher $[Ca^{2+}]_i$ levels. For the Ca^{2+}-binding ratio of Fura-2 the dependence on $[Ca^{2+}]_i$ was taken into account by using the incremental Ca^{2+}- binding ratio κ'_B (Eq. 1).

Calcium binding to Fura-2 and cytoplasmic Ca^{2+}-binding proteins occurs within milliseconds (Neher, 1995); therefore the assumption of rapid local chemical equilibration is likely to hold. The measurements of the decay time constants of the $[Ca^{2+}]_i$ transients using Fura-2 were not limited by its estimated off rate of 150 s^{-1} ($k_{on} \approx 6 \times 10^8\ M^{-1} \cdot s^{-1}$; Kao and Tsien, 1988; $K_d \approx 260$ nM), because the fastest decays measured had time constants of 100–150 ms. On the other hand, the decay time constants we measured using low-affinity indicators were so fast (<50 ms) that a strict separation between diffusional equilibration and extrusion of Ca^{2+} may not be possible (Neher, 1995). Although $[Ca^{2+}]_i$ presumably equilibrates rapidly within a terminal thickness of r = 1–2 μm (characteristic time $r^2/6D_{Ca}$ is about 3–13 ms, assuming an effective Ca^{2+} diffusion constant D_{Ca} of 50 $\mu m^2 \cdot s^{-1}$), there might exist lateral $[Ca^{2+}]_i$ gradients that dissipate more slowly. Therefore we discuss the assumption of spatial homogeneity here in more detail.

For simplicity we write $c_f(\mathbf{x}, t)$ for the spatially dependent free calcium concentration $\Delta[Ca^{2+}]_i$ $(\mathbf{x}, t)$ with $\mathbf{x} = (x, y, z)$. We assume rapid local chemical equilibrium of calcium with the mobile Ca^{2+} buffers S and B, and a spatially homogeneous linear Ca^{2+} extrusion with rate γ. If the diffusion constants of the free and the bound forms of the buffers are assumed to be equal, then the spatiotemporal distribution of free calcium after an action potential is described by the differential equation (Wagner and Keizer, 1994)

$$\frac{\partial c_f(\mathbf{x}, t)}{\partial t}(1 + \kappa_S + \kappa_B) = \left\{\sum_i D_i \nabla(\nabla c_i(\mathbf{x}, t))\right\} - \gamma c_f(\mathbf{x}, t). \tag{A1}$$

The summation runs over free calcium and the bound forms of calcium with the corresponding diffusion constants. The volume-averaged free Ca^{2+} concentration is defined as

$$\overline{c_f(t)} = \frac{1}{V}\int_V dx^3\, c_f(\mathbf{x}, t), \tag{A2}$$

with the accessible volume V. Integrating Eq. A1 over V and exchanging integration and differentiation on the left side yields

$$\frac{\partial \overline{c_f(t)}}{\partial t}(1 + \kappa_S + \kappa_B) = \left\{\sum_i \frac{D_i}{V}\int_V dx^3\, \nabla(\nabla c_i(\mathbf{x}, t))\right\} - \gamma \overline{c_f(t)}. \tag{A3}$$

Using Gauss's law, the volume integrals can be converted to surface integrals

$$\frac{\partial \overline{c_f(t)}}{\partial t}(1 + \kappa_S + \kappa_B) = \left\{\sum_i \frac{D_i}{V}\oint_S dn(\nabla c_i(\mathbf{x}, t))_n\right\} - \gamma \overline{c_f(t)}, \tag{A4}$$

where S corresponds to all surface membranes of the cytoplasm and $(\nabla c_i(\mathbf{x}, t))_n$ is the normal component of the concentration gradient of free or bound calcium at the surface. The cell membranes are considered to be reflective walls, i.e., impermeable for calcium ions and buffer molecules. Therefore $(\nabla c_i(\mathbf{x}, t))_n$ is zero and the surface integrals vanish. Thus Eq. A4 reduces to the simple differential equation of the single compartment model for the volume-averaged $\Delta[Ca^{2+}]_i$. The model even holds under conditions of a persisting Ca^{2+} concentration gradient within the volume, provided the pump is linear and homogeneously distributed within the terminal volume. With respect to possible lateral Ca^{2+} gradients in the calyx, this means that Ca^{2+} removal should follow a similar (exponential) time course in the different parts of the terminal. Consistent with this idea, the Ca^{2+} signals in the preterminal axon and in the calyx followed a similar time course, despite a large concentration gradient between them (Borst et al., 1995).

We thank Dr. E. Neher for discussions and helpful comments on the manuscript, Drs. L. P. Wollmuth and L.-G. Wu for critically reading the manuscript, and M. Kaiser for expert technical assistance.

JGGB was supported by E.U. (TMR program).

REFERENCES

Adler, E. M., G. J. Augustine, S. N. Duffy, and M. P. Charlton. 1991. Alien intracellular calcium chelators attenuate neurotransmitter release at the squid giant synapse. *J. Neurosci.* 11:1496–1507.

Agard, D. A., Y. Hiraoka, P. Shaw, and J. W. Sedat. 1989. Fluorescence microscopy in three dimensions. *Methods Cell Biol.* 30:353–376.

Augustine, G. J., and M. P. Charlton. 1986. Calcium dependence of presynaptic calcium current and post-synaptic response at the squid giant synapse. *J. Physiol. (Lond.).* 381:619–640.

Augustine, G. J., and E. Neher. 1992. Neuronal Ca^{2+} signalling takes the local route. *Curr. Opin. Neurobiol.* 2:302–307.

Barnes-Davies, M., and I. D. Forsythe. 1995. Pre- and postsynaptic glutamate receptors at a giant excitatory synapse in rat auditory brainstem slices. *J. Physiol. (Lond.).* 488:387–406.

Blaustein, M. P. 1988. Calcium transport and buffering in neurons. *Trends Neurosci.* 11:438–443.

Borst, J. G. G., F. Helmchen, and B. Sakmann. 1995. Pre- and postsynaptic whole-cell recordings in the medial nucleus of the trapezoid body of the rat. *J. Physiol. (Lond.).* 489:825–840.

Borst, J. G. G., and B. Sakmann. 1996. Calcium influx and transmitter release in a fast CNS synapse. *Nature.* 383:431–434.

Brinley, F. J. 1978. Calcium buffering in squid axon. *Annu. Rev. Biophys. Bioeng.* 7:363–392.

Erhardt, A., G. Zinser, D. Komitowski, and J. Bille. 1984. Reconstructing 3-D light-microscopic images by digital image processing. *Appl. Optics.* 24:194–200.

Escobar, A. L., J. R. Monck, J. M. Fernandez, and J. L. Vergara. 1994. Localization of the site of Ca^{2+} release at the level of a single sarcomere in skeletal muscle fibres. *Nature.* 367:739–741.

Fogelson, A. L., and R. S. Zucker. 1985. Presynaptic calcium diffusion from various arrays of single channels: implications for transmitter release and synaptic facilitation. *Biophys. J.* 48:1003–1017.

Forsythe, I. D. 1994. Direct patch recording from identified presynaptic terminals mediating glutamatergic EPSCs in the rat CNS, in vitro. *J. Physiol. (Lond.).* 479:381–387.

Friauf, E. 1993. Transient appearance of calbindin-D28k-positive neurons in the superior olivary complex of developing rats. *J. Comp. Neurol.* 334:59–74.

Groden, D. L., Z. Guan, and B. T. Stokes. 1991. Determination of Fura-2 dissociation constants following adjustment of the apparent Ca-EGTA association constant for temperature and ionic strength. *Cell Calcium.* 12:279–287.

Grynkiewicz, G., M. Poenie, and R. Y. Tsien. 1985. A new generation of Ca^{2+} indicators with greatly improved fluorescence properties. *J. Biol. Chem.* 260:3440–3450.

Helmchen, F., K. Imoto, and B. Sakmann. 1996. Ca^{2+} buffering and action potential-evoked Ca^{2+} signaling in dendrites of pyramidal neurons. *Biophys. J.* 70:1069–1081.

Herrington, J., and R. J. Bookman. 1994. Pulse Control V4.0: IGOR XOPs for Patch Clamp Data Acquisition and Capacitance Measurements. University of Miami, Miami, FL.

Jackson, M. B., A. Konnerth, and G. J. Augustine. 1991. Action potential broadening and frequency-dependent facilitation of calcium signals in pituitary nerve terminals. *Proc. Natl. Acad. Sci. USA.* 88:380–384.

Jaffe, D. B., D. Johnston, N. Lasser-Ross, J. E. Lisman, H. Miyakawa, and W. N. Ross. 1992. The spread of Na^+ spikes determines the pattern of dendritic Ca^{2+} entry into hippocampal neurons. *Nature.* 357:244–246.

Kao, J. P. Y., and R. Y. Tsien. 1988. Ca^{2+} binding kinetics of fura-2 and azo-1 from temperature-jump relaxation measurements. *Biophys. J.* 53: 635–639.

Konishi, M., and J. R. Berlin. 1993. Ca transients in cardiac myocytes measured with a low affinity fluorescent indicator, furaptra. *Biophys. J.* 64:1331–1343.

Llinás, R., M. Sugimori, and R. B. Silver. 1992. Microdomains of high calcium concentration in a presynaptic terminal. *Science.* 256:677–679.

Llinás, R., M. Sugimori, and S. M. Simon. 1982. Transmission by presynaptic spike-like depolarization in the squid giant synapse. *Proc. Natl. Acad. Sci. USA.* 79:2415–2419.

Lohmann, C., and E. Friauf. 1996. Distribution of the calcium-binding proteins parvalbumin and calretinin in the auditory brainstem of adult and developing rats. *J. Comp. Neurol.* 367:90–109.

Martinez-Serrano, A., P. Blanco, and J. Satrústegui. 1992. Calcium binding to the cytosol and calcium extrusion mechanisms in intact synaptosomes and their alteration with aging. *J. Biol. Chem.* 267:4672–4679.

Mintz, I. M., B. L. Sabatini, and W. G. Regehr. 1995. Calcium control of transmitter release at a central synapse. *Neuron.* 15:675–688.

Morest, D. K. 1968. The growth of synaptic endings in the mammalian brain: a study of the calyces of the trapezoid body. *Z. Anat. Entwicklungsgesch.* 127:201–220.

Neher, E. 1995. The use of fura-2 for estimating Ca buffers and Ca fluxes. *Neuropharmacology.* 34:1423–1442.

Neher, E., and G. J. Augustine. 1992. Calcium gradients and buffers in bovine chromaffin cells. *J. Physiol. (Lond.).* 450:273–301.

Neher, E., and R. S. Zucker. 1993. Multiple calcium-dependent processes related to secretion in bovine chromaffin cells. *Neuron.* 10:21–30.

Oliva, C., I. S. Cohen, and R. T. Mathias. 1988. Calculation of time constants for intracellular diffusion in whole cell patch clamp configuration. *Biophys. J.* 54:791–799.

Regehr, W. G., and P. Atluri. 1995. Calcium transients in cerebellar granule cell presynaptic terminals. *Biophys. J.* 68:2156–2170.

Regehr, W. G., K. R. Delaney, and D. W. Tank. 1994. The role of presynaptic calcium in short-term enhancement at the hippocampal mossy fiber synapse. *J. Neurosci.* 14:523–537.

Regehr, W. G., and D. W. Tank. 1991. The maintenance of LTP at hippocampal mossy fiber synapses is independent of sustained presynaptic calcium. *Neuron.* 7:451–459.

Reuter, H., and H. Porzig. 1995. Localization and functional significance of the Na^+/Ca^{2+} exchanger in presynaptic boutons of hippocampal cells in culture. *Neuron.* 15:1077–1084.

Roberts, W. M. 1994. Localization of calcium signals by a mobile calcium buffer in frog saccular hair cells. *J. Neurosci.* 14:3246–3262.

Sala, F., and A. Hernández-Cruz. 1990. Calcium diffusion in a spherical neuron: relevance of buffering properties. *Biophys. J.* 57:313–324.

Schneggenburger, R., Z. Zhou, A. Konnerth, and E. Neher. 1993. Fractional contribution of calcium to the cation current through glutamate receptor channels. *Neuron.* 11:133–143.

Schweizer, F. E., H. Betz, and G. J. Augustine. 1995. From vesicle docking to endocytosis: intermediate reactions of exocytosis. *Neuron.* 14: 689–696.

Simon, S. M., and R. R. Llinás. 1985. Compartmentalization of the submembrane calcium activity during calcium influx and its significance in transmitter release. *Biophys. J.* 48:485–498.

Sinha, S. R., L.-G. Wu, and P. Saggau. 1997. Presynaptic calcium dynamics and transmitter release evoked by single action potentials at mammalian central synapses. *Biophys. J.* 72:637–651.

Smith, S. J., and G. J. Augustine. 1988. Calcium ions, active zones and synaptic transmitter release. *Trends Neurosci.* 11:458–464.

Stuart, G. J., H.-U. Dodt, and B. Sakmann. 1993. Patch-clamp recordings from the soma and dendrites of neurons in brain slices using infrared video microscopy. *Pflügers Arch.* 423:511–518.

Stuenkel, E. L. 1994. Regulation of intracellular calcium and calcium buffering properties of rat isolated neurohypophysial nerve endings. *J. Physiol. (Lond.).* 481:251–271.

Tank, D. W., W. G. Regehr, and K. R. Delaney. 1995. A quantitative analysis of presynaptic calcium dynamics that contribute to short-term enhancement. *J. Neurosci.* 15:7940–7952.

Ukhanov, K. Y., T. M. Flores, H.-S. Hsiao, P. Mohapatra, C. H. Pitts, and R. Payne. 1995. Measurements of cytosolic Ca^{2+} concentration in *Limulus* ventral photoreceptors using fluorescent dyes. *J. Gen. Physiol.* 105: 95–116.

Wagner, J., and J. Keizer. 1994. Effects of rapid buffers on Ca^{2+} diffusion and Ca^{2+} oscillations. *Biophys. J.* 67:447–456.

Wu, L.-G., and P. Saggau. 1994. Pharmacological identification of two types of presynaptic voltage-dependent calcium channels at CA3-CA1 synapses of the hippocampus. *J. Neurosci.* 14:5613–5622.

Zhao, M., S. Hollingworth, and S. M. Baylor. 1996. Properties of tri- and tetracarboxylate Ca^{2+} indicators in frog skeletal muscle fibers. *Biophys. J.* 70:896–916.

Zhou, Z., and S. Misler. 1995. Action potential-induced quantal secretion of catecholamines from rat adrenal chromaffin cells. *J. Biol. Chem.* 270:3498–3505.

Zucker, R. S. 1994. Calcium and short-term synaptic plasticity. *Neth. J. Zool.* 44:495–512.